Unified Performance Theory for V/STOL Aircraft in Equilibrium Flight. Part I

T. STRAND,* E. S. LEVINSKY,† AND M. H. Y. WEI‡
Air Vehicle Corporation, La Jolla, Calif.

A V/STOL theory for equilibrium level flight is presented which unifies the calculation of optimum performance over the complete velocity spectrum from hover to cruise. The theory has been correlated with existing test results on a number of different V/STOL aircraft by presenting lift/drag and nondimensional power-required curves vs nondimensional velocity. In general, realistic agreement between theory and experiment is found over the entire velocity range.

Nomenclature

A = a constant
A_n = Fourier coefficients
A_s = sum of the fully contracted slipstream areas behind propellers or of the geometric exit areas of ducted propellers or fans
AR = aspect ratio ($= b^2/S$)
BHP = brake (shaft) horse power ($= P/\eta\ 550$)
b = wing span
C = parameter; also a constant
C_L = airplane lift coefficient ($= L/qS$)
C_D = airplane drag coefficient ($= D/qS$)
D = airplane drag; also a constant
e = wing aerodynamic effectiveness
F = incomplete elliptic integral of the first kind; also complex potential function
f = equivalent flat-plate drag area ($= D_0/q = C_{D0}S$); also complex potential function
H = propeller in-plane force; also complex potential function for flow outside slipstreams
h = complex potential function for flow inside slipstreams; also a length
i = $(-1)^{1/2}$
K = complete elliptic integral of the first kind
k = modulus of K
k' = $(1 - k^2)^{1/2}$
L, l = airplane total, local lift
$\dot{m}$ = mass flow rate, slugs/sec
n = normal direction, positive into the fluid under consideration
P = power required ($= \eta\ 550$ BHP); also length of wingtip outboard of slipstream
p = velocity ratio V_∞/V_s
Q_{pr} = propeller torque due to zero-lift blade drag
q = dynamic pressure ($= \frac{1}{2}\rho V^2$)
R = propeller force normal to disk; also radius of duct or propeller slipstream
r = radial distance
S = wing planform area, also conformal mapping plane
s = direction tangent to vortex boundary; also a length
T = kinetic energy per unit strip in the longitudinal vortex direction; also propeller horizontal force in "two-dimensional" flow [$= \dot{m}_p(V_s - V_\infty)$]
t = dummy variable of integration
V = velocity
v = uniform induced velocity in and normal to the plane of the propeller; also sidewash velocity
W = airplane weight
w = downwash velocity
y = coordinate
y_0 = distance along abscissa
Z = complex variable ($= y + iz$)
z = coordinate
β = angle of the fully developed slipstream, measured from the vertical direction
∂ = partial derivative
δ = angle of the fully developed slipstream, measured from the horizontal direction
ϵ = angle of the vortex sheet, measured from the positive direction of the oncoming stream
Γ = circulation
ζ = complex variable ($= \xi + i\eta$)
η = propeller efficiency; also coordinate
θ = propeller angle of tilt, or angle in mapping plane
λ_s = $\dfrac{1 - (V_\infty/V_s)^2}{1 + (V_\infty/V_s)^2}$
μ = coordinate
ν = coordinate
ξ = coordinate
ρ = air density
Σ = cross-sectional area associated with apparent mass
Φ = velocity potential
φ = velocity potential
ψ = stream function
Ω = rotational speed, cps

Subscripts

b = boundary
eff = effective
h = hover
i = induced, or image
∞ = refers to conditions at infinity or to the outside flow
max = maximum
0 = zero lift
p = propeller
s = slipstream
w = wing

Received June 1, 1966; revision received November 23, 1966. The research was carried out under the direction of the Aerodynamics Laboratory, David Taylor Model Basin, U. S. Navy, on Contract Nonr-4926(00)(X). The authors wish to acknowledge several helpful discussions with H. Chaplin of the David Taylor Model Basin relating to the problems treated in the paper. They are also indebted to H. M. Grijalva for computations and preparation of the graphs. [3.01]

* President. Associate Fellow AIAA.
† Vice President. Member AIAA.
‡ Staff Scientist.

1. Introduction

A SIMPLE unified V/STOL performance theory for equilibrium flight at all forward speeds is presently lacking. Our objective here is to present such a theory by which lift, drag, and power required can be easily and rapidly calculated with reasonable accuracy for all flight speeds, based upon the condition of minimum induced drag for a given airplane weight. The thought behind this development may be stated in the following concise form.

To a useful degree of approximation an airplane—be it rotary wing, conventional fixed wing, or any of the known VTOL or STOL types—can be entirely characterized for fundamental performance evaluation purposes by its weight and the following three areas: 1) a cross-sectional area

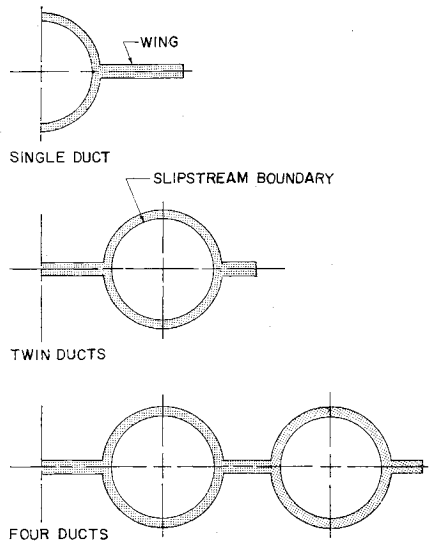

Fig. 1 Three general types of V/STOL configurations with wing and ducted propellers or fans (rear view at cruise).

Σ, associated with the Trefftz-plane apparent (virtual) mass of the configuration, which for the specific case of a monoplane wing in the absence of slipstreams is equal to $\pi b^2/4$, where b is the span of the airplane; 2) a slipstream cross-sectional area A, defined as the sum of the fully contracted slipstream areas behind propellers, or as the sum of the geometric exhaust areas of jets, ducted fans, or shrouded propellers; and 3) a "dissipation area" f, which is sometimes called the "equivalent flat plate drag area," and which is determined by the airplane skin friction and parasite drag.

The subsequent development applies to those types of V/STOL aircraft that exhibit a relatively simple interaction between the wing and the propulsion units. Included are aircraft with ducted propellers or fans (jets) and all tilt-wing and deflected slipstream types. Excluded from consideration are brute force vehicles such as the direct lift aircraft. Excluded are also the fan-in-wing types, the interaction of which is presently beyond theoretical analysis.

Performance data of V/STOL aircraft seem to be most universally available in the form of power required vs speed. The unified theory presented here permits one to deduce the effectiveness of the aerodynamic systems throughout the speed range by analysis of the power required curve. It will be assumed throughout that the wake does not roll up, and that separation does not occur.

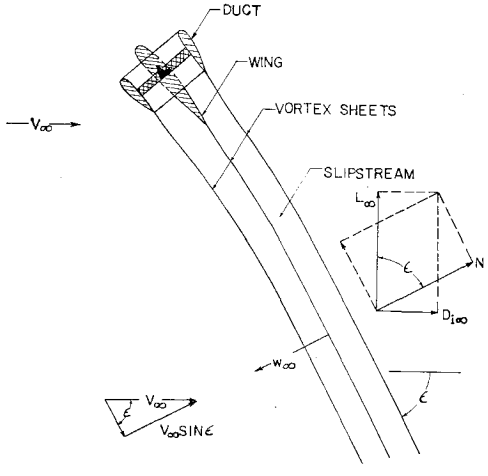

Fig. 2 Forces, velocities, and wake deflection for wing and duct combinations (side view).

2. Performance Theory

2.1 Wing with Ducted Propellers or Fans

Let us consider a V/STOL airplane configuration with one or more ducted propellers or fan engines mounted in the plane of the wing (Fig. 1). Munk[1] showed that for minimum induced drag, the downwash must assume constant values throughout a perpendicular section of the wake at infinity downstream. An upstream view of the wake in our case shows a straight vortex sheet originating from the wings and joined to circular peripheral sheets from the ducts. The individual vortex lines are deflected downward. This deflection is caused by self-induction, i.e., the combined effect of all the vortices on an arbitrary vortex is to cause it to move at a velocity w_∞ normal to itself. The vortex system bends downward until an angle ϵ is reached The induced velocity w_∞ is then equal and opposite to the component $V_\infty \sin\epsilon$ of the freestream, and a stable condition is reached (Fig. 2).

In the present development we shall employ finite-span wing theory associated with large downwash angles. This theory has been discussed by Helmbold,[2] Ribner,[3] McCormick,[4] Hancock,[5] Davenport,[6] and Cone.[7] The theory is at present insufficiently corroborated by test results. It is, however, the only one available, except for a recent suggestion by Graham[8] that the curvature of the wing wake might also have to be taken into consideration. The other investigators just mentioned all assume the wake to be straight. The existing theory will be augmented by considering the effects of slipstreams or jets. For monoplane wings without slipstreams or jets, the expressions found will reduce to those given by Ribner. They also may be deduced easily from Helmbold's note.

The total airplane weight W may be expressed as a sum of the lift from apparent mass concepts (due to the solid obstacle moving normal to itself with the velocity $V_\infty \sin\epsilon$), which we shall denote by L_∞, and that due to momentum transfer in the slipstream through a momentum control surface at infinity downstream, i.e.,

$$W = L_\infty + \dot{m}_s V_s \sin\epsilon \tag{1}$$

Here $\dot{m}_s$ and V_s are the slipstream mass flow rate and velocity, respectively.

Similarly, for level equilibrium flight the horizontal forces must balance, and we may write

$$D_{i\infty} + D_0 = \dot{m}_s(V_s \cos\epsilon - V_\infty) \tag{2}$$

$D_{i\infty}$ and D_0 are, respectively, the induced drag associated with apparent mass concepts and the skin-friction (including parasite) drag. The power required P may be written as follows:

$$P = \tfrac{1}{2}\dot{m}_s(V_s^2 - V_\infty^2) \tag{3}$$

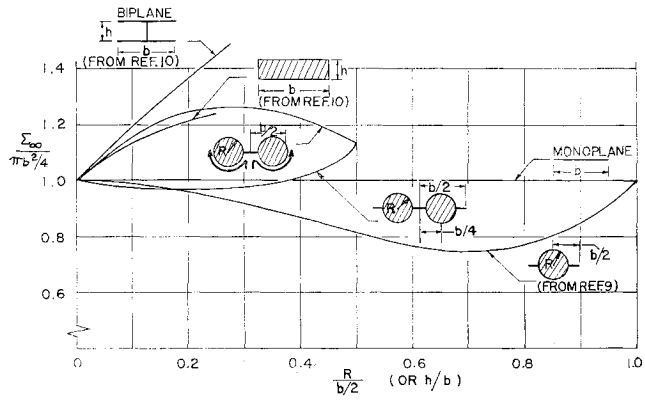

Fig. 3 Summary graph of cross-sectional areas associated with apparent mass of duct and wing combinations.

Equations (1–3) are the basic relations required for performance calculations involving any ducted propeller, fan, or jet configuration.

By momentum considerations it can be shown that

$$L_\infty = q_\infty \Sigma_\infty (2 - \sin^2\epsilon) \sin\epsilon \quad (4)$$

$$D_{i\infty} = q_\infty \Sigma_\infty \sin^2\epsilon \cos\epsilon \quad (5)$$

Here Σ_∞ is a cross-sectional area associated with apparent mass. For a monoplane wing without slipstreams, it is equal to $\pi b^2/4$. A summary graph of Σ_∞ is presented in Fig. 3. Ribner's results are obtained if $\Sigma_\infty = \pi b^2/4$, i.e., if we have a monoplane wing. The expressions are supposedly valid for all wake angles, including the case when $\epsilon = 90°$. Both the apparent mass lift and induced drag are then equal to zero, since $\epsilon = 90°$ corresponds to hovering flight, i.e., q_∞ is zero for equilibrium.

To take into account the fact that the downwash at infinity is not exactly constant, and to make allowance for other losses such as those due to local flow separation and other viscous effects, it is proposed to include the usual effectiveness factor e by multiplication into Σ_∞.

Solving Eq. (1) for the slipstream velocity with $\dot{m}_s = \rho V_s A_s$, where A_s denotes the sum of the slipstream cross-sectional areas, and defining $p = V_\infty/V_s$, we find

$$V_s^2 = \frac{2W}{\rho \sin\epsilon [p^2 \Sigma_\infty e(2 - \sin^2\epsilon) + 2A_s]} \quad (6)$$

At cruise speeds $V_s \to V_\infty$, and ϵ is a small angle. In this case Eq. (6) may be solved for ϵ, to yield

$$\epsilon = \frac{2C_L}{\pi AR(\Sigma_\infty e + A_s)/(\pi b^2/4)} \quad (7)$$

Thus in aircraft design it is desirable to select the configuration with the largest Σ_∞, all other parameters being equal. It is also apparent that ducted configurations are quite advantageous as far as induced drag is concerned, since from Fig. 3, Σ_∞ is by itself almost always equal to or larger than $\pi b^2/4$. In the previous expression, the sum of Σ_∞ and A_s are for practical configurations always larger than $\pi b^2/4$. It should also be noted from Fig. 3 that it is beneficial to locate the ducts as far out towards the wing tips as possible.

Similarly, Eq. (2) may be solved for the nondimensional velocity ratio

$$p = [(1 + 2C\cos\epsilon)^{1/2} - 1]/C \quad (8)$$

where, if by definition $f = C_{D_0} S$, with C_{D_0} and S being, respectively, the skin-friction coefficient and the wing reference area, we have

$$C = (\Sigma_\infty e/A_s) \sin^2\epsilon \cos\epsilon + f/A_s \quad (9)$$

We note that $V_\infty/V_h = p(V_s/V_h)$, where $V_h = (W/\rho A_s)^{1/2}$ by definition. Thus from Eq. (6) the nondimensional velocity becomes

$$\frac{V_\infty}{V_h} = \frac{2^{1/2} p}{\sin^{1/2}\epsilon [p^2(\Sigma_\infty e/A_s)(2 - \sin^2\epsilon) + 2]^{1/2}} \quad (10)$$

Then, dividing through in Eq. (3) by the hover power $[P_h = W^{3/2}/2(\rho A_s)^{1/2}]$, we find

$$\mathrm{BHP}/\mathrm{BHP}_h = [\eta_h(1 - p^2)/\eta p^3][V_\infty/V_h]^3 \quad (11)$$

Here η_h and η denote, respectively, the propeller or fan efficiency at hover (usually called the figure of merit) and at forward velocity V_∞. It should be noted that these are propeller efficiencies only (propulsive divided by the ideal efficiency). The ideal efficiency has been taken care of by our use of V_s as one of the basic parameters.

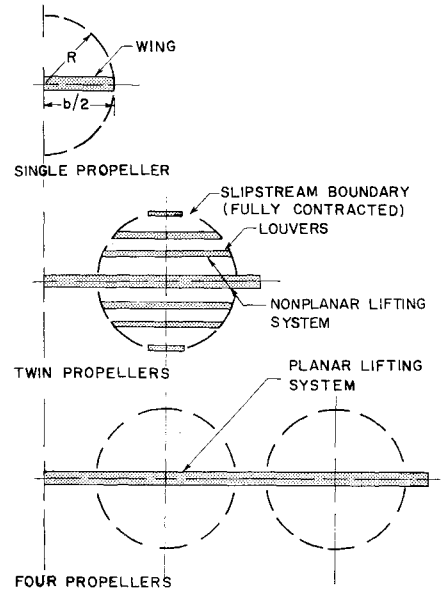

Fig. 4 Three general types of V/STOL configurations with monoplane wing and unshrouded propellers (rear view at cruise).

An effective lift/drag ratio may also be calculated as a function of the nondimensional flight speed by noting that

$$\left(\frac{L}{D}\right)_{\mathrm{eff}} = \frac{W \cdot V_\infty}{D \cdot V_\infty} = \frac{2\eta_h V_\infty/V_h}{\eta\ \mathrm{BHP}/\mathrm{BHP}_h} \quad (12)$$

This equation is easily interpreted geometrically on a curve of nondimensional power vs velocity as $(2\eta_h/\eta)$ divided by the tangent of the angle between the abscissa and a line from the origin to any point on the curve. Results of numerical calculations using these equations are given in Sec. 3.

2.2 Wing with Unshrouded Propellers

The unshrouded propellers will be considered to act independently of the wing with a lift and thrust based on their tilt angle. The propeller slipstream will be assumed to be fully contracted and fully deflected when it crosses the wing. The wing may then further deflect the slipstream and the outside flow downward, subject to the optimum condition[16,22] that the resultant downwash *angle* be constant along the trailing vortex sheet. However, depending on the flap characteristics, the slipstream may or may not be deflected as a solid body (see Sec. 2.2.2).

The aerodynamic problems associated with a wing placed in slipstreams have been investigated by many authors.[11–21] In spite of this the problem has largely resisted successful solution. We have chosen to approach a solution by starting from the two end points on the velocity scale, namely $V_\infty = V_s$ and $V_\infty = 0$, and working towards intermediate values of the velocity. Satisfactory solutions can be obtained around each of the two end points for the case of minimum induced drag for a given lift. A theory is then proposed for the intermediate transitional flight regime, which reduces to the proper limits at both end points and permits the minimum power requirements to be calculated over the entire velocity region with a single set of equations. Monoplane wings with single, two, and four propellers will be considered (see Fig. 4).

2.2.1 Inclined propeller alone

To allow determination of the optimum division of lift between propeller and wing, a propeller theory, which is applicable to inclined lifting propellers, is required. We shall use rotor theory, which may be regarded as an extension of

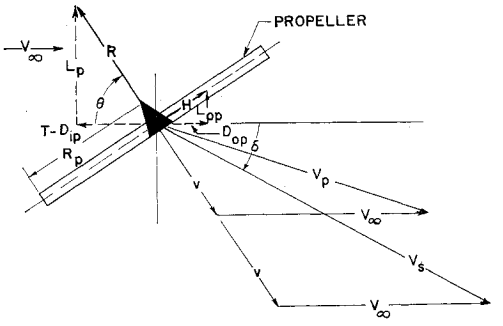

Fig. 5 Inclined propeller alone.

simple momentum theory, and is based upon an assumption by Glauert for which no proof or disproof exists. Glauert's rotor theory yields momentum theory at both end points of the velocity scale.

If R denotes the resultant force on the propeller, acting normal to the propeller disk, Glauert's assumption for the uniform induced velocity v at the rotor states that

$$v = R/2\rho V_p A_p \tag{13}$$

with A_p and V_p being the propeller disk area and the resultant velocity at the disk, respectively. From the velocity vector diagram given in Fig. 5, it is easily seen that

$$v = (V_p^2 - V_\infty^2 \sin^2\theta)^{1/2} - V_\infty \cos\theta \tag{14}$$

where θ is the propeller inclination angle measured from the horizontal direction.

To determine the flow conditions at the wing, which is assumed to be operating in the fully contracted slipstream, we shall require an expression for the relation between the flow velocity V_p at the propeller and the velocity V_s inside the fully contracted slipstream. Referring back to Fig. 5, we find

$$2v/V_s = (1 - p^2 \sin^2\theta)^{1/2} - p\cos\theta \tag{15}$$

Elimination of v between Eqs. (14) and (15) yields the desired relation

$$V_p/V_s = \tfrac{1}{2}[1 + p^2(1 + 2\sin^2\theta) + 2p\cos\theta(1 - p^2\sin^2\theta)^{1/2}]^{1/2} \tag{16}$$

Here $p = V_\infty/V_s$ by definition. At cruise, where $p \simeq 1$ and $\theta \simeq 0$, this reduces to the simple momentum theory result $V_p/V_s = (1 + p)/2$. At hover $V_p/V_s = \tfrac{1}{2}$.

The power required for an inclined propeller is given by the usual expression

$$P = \tfrac{1}{2}\dot{m}_p(V_s^2 - V_\infty^2) \tag{17}$$

The mass flow $\dot{m}_p$ is, however, not equal to $\dot{m}_s$ as obtained from simple momentum theory, but is instead equal to $(\rho V_p A_p)$. This is Glauert's fundamental hypothesis. An equivalent expression for power is $R(v + V_\infty \cos\theta)$, of which the product Rv is usually termed the induced power required.

The propeller lift is now $R\sin\theta$, and the horizontal force component equals $R\cos\theta$, where from Eq. (13)

$$R = 2q_s[2v/V_s][V_p/V_s]A_p \tag{18}$$

The terms in brackets are given by Eqs. (15) and (16).

In subsequent sections we shall find it more convenient in some cases to work with the deflection angle δ of the fully contracted slipstream instead of the propeller inclination angle θ. It follows from Fig. 5 that

$$\sin\delta = \sin\theta[(1 - p^2\sin^2\theta)^{1/2} - p\cos\theta] \tag{19}$$

$$\cos\delta = p + \cos\theta[(1 - p^2\sin^2\theta)^{1/2} - p\cos\theta] \tag{20}$$

Denoting the vertical and horizontal components of the propeller normal force by L_p and $R\cos\theta$, respectively, we may easily prove that

$$L_p = R\sin\theta = \dot{m}_p V_s \sin\delta \tag{21}$$

and

$$R\cos\theta = \dot{m}_p(V_s\cos\delta - V_\infty) = T - D_{ip} \tag{22}$$

where by definition $T = \dot{m}_p(V_s - V_\infty)$ and $D_{ip} = \dot{m}_p V_s(1 - \cos\delta)$.

When a propeller or rotor is translating, there is also an in-plane force acting on it and opposing the motion. A first estimate of the magnitude of this force, which we shall call H (see Fig. 5), may be determined by integrating the average zero-lift drag coefficient C_{d0} over the blade. In the subsequent development we shall assume that H is small and can be neglected.

Denoting the torque due to zero-lift blade drag by Q_{pr}, we may define a new propeller efficiency for V/STOL aircraft as follows:

$$\eta = \frac{\tfrac{1}{2}\dot{m}_p(V_s^2 - V_\infty^2)}{\tfrac{1}{2}\dot{m}_p(V_s^2 - V_\infty^2) + \Omega Q_{pr} + P_s} \tag{23}$$

where P_s is the additional power required because of zero-lift slipstream overspeed effects on the wing-flap system. This expression reduces to the figure of merit η_h at zero forward speed and, when P_s is negligible, becomes the conventional propeller efficiency (propulsive efficiency divided by the ideal efficiency) at cruise conditions. It can be shown that P_s is given by

$$P_s = (f_s/A_s)\dot{m}_p(V_s^2 - V_\infty^2)/2 \qquad \text{for } f_s \ll A_s \tag{24}$$

Here f_s is the equivalent flat-plate drag area inside the slipstream.

2.2.2 Wing and propeller combinations at cruise and upper transition speeds

Consider a monoplane V/STOL airplane having one or more unshrouded propellers mounted ahead of the wing. It will be assumed that the deflection of the propeller slipstream far behind the propeller is so small at cruise and upper transition speeds that the wing-propeller theory of Squire and Chester, which is based on uninclined slipstreams, may be employed. In the optimum case, when the wing causes the vortex sheet far downstream to trail downward at a constant angle ϵ, the equations of equilibrium flight become

$$W = \rho e\Sigma_\infty V_\infty^2\epsilon + \rho e\Sigma_s V_s^2\epsilon = \rho e[\Sigma_\infty + \Sigma_s/p^2]V_\infty^2\epsilon, \tag{25}$$

$$\dot{m}_p(V_s - V_\infty) = \rho e\Sigma_\infty V_\infty^2\epsilon^2/2 + \rho e\Sigma_s V_s^2\epsilon^2/2 + fq_\infty = \rho e[\Sigma_\infty + \Sigma_s/p^2]V_\infty^2\epsilon^2/2 + fq_\infty \tag{26}$$

Here Σ_∞ and Σ_s are the cross-sectional areas associated with the apparent mass in the Trefftz plane for the outside (free-stream) and inside (slipstream) flow, respectively. The equivalent flat-plate area $f = C_{D_0}S$ pertains to the flow both inside and outside the slipstream, and is based upon V_∞, since overspeed effects are included in the propeller efficiency.

The detailed calculation of Σ_∞ and Σ_s for tilt-wing and deflected slipstream aircraft is presented in Sec. B of Pt. II.§ It is shown that Σ_∞ and Σ_s are functions not only of the aircraft geometry as in the case of ducted propeller aircraft, but also of V_∞/V_s. In addition, it is clear that they will also be a function of the type of wing flap or turning vanes employed. If ducts or louvered flaps (nonplanar deflection devices) are used, whose shed vorticity

§ To be published in a future issue of the Journal of Aircraft.

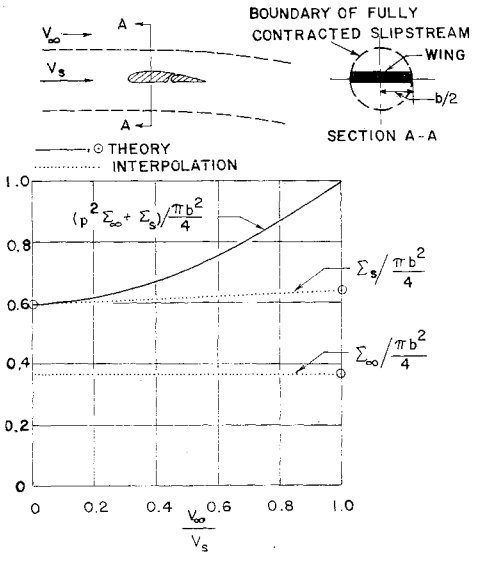

Fig. 6a Cross-sectional areas associated with apparent mass of a single unshrouded propeller and wing combination with the wing spanning the fully contracted slipstream.

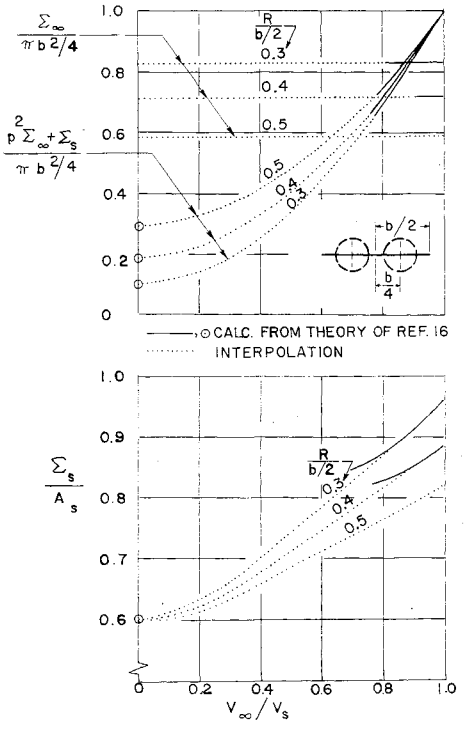

Fig. 6b Cross-sectional areas associated with apparent mass of twin propeller and wing combinations.

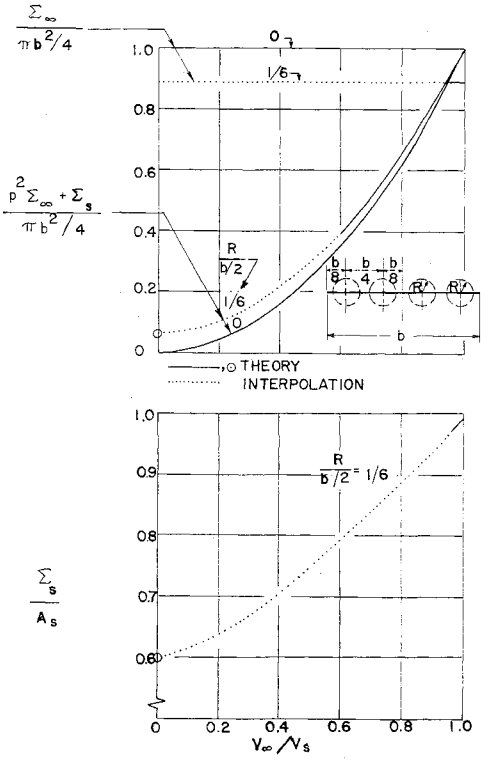

Fig. 6c Cross-sectional areas associated with apparent mass of four propeller and wing combinations.

either surrounds the slipstream or is distributed across it in the optimum manner, then the entire slipstream will move downward at a constant angle equal to the wing downwash angle. In this case Σ_s will be a maximum and equal to the cross-sectional area A_s of the fully contracted slipstreams. Σ_∞ will then also be identical to that of a ducted propeller configuration of the same geometry in the Trefftz plane. If, on the other hand, the shed vorticity is confined to the plane of the wing, then there is no vortex sheet surrounding the slipstream, and it is no longer possible to deflect the entire slipstream downward through a constant angle ϵ. Of course, the vortex sheet itself must still be deflected a constant angle ϵ, inside as well as outside the slipstream, in accordance with the optimization criterion. The average deflection angle of the fluid particles in the slipstream at infinity downstream is now less than ϵ. This fact lowers Σ_s to a value below A_s. The apparent mass of the flow outside the slipstreams will in general also be reduced when the shed vorticity is confined to a single plane.

We thus distinguish between two types of unshrouded propeller and wing combinations having a constant downwash angle at infinity downstream. The most efficient type, yielding the largest Σ, has louvered flaps or ducts (see Sec. 2.1 and Sec. A of Pt. II¶). The least efficient type is the one with a planar lifting surface (monoplane wing). Summary graphs for Σ_∞ and Σ_s for the latter type are given in Fig. 6. The theory is developed in Sec. B of Pt. II. Monoplane flap configurations probably may be classified as falling in between these two cases, since large double- or triple-slotted flaps are essentially nonplanar in a rear view. Practical flaps might, of course, still not perform as well as Fig. 6 predicts, because the downwash angle might not be constant along the span.

From Eqs. (25) and (26) the vortex wake angle at infinity downstream and the induced-drag coefficient may be expressed as follows:

$$\epsilon = \frac{2C_L}{\pi ARe(\Sigma_\infty + \Sigma_s/p^2)/(\pi b^2/4)} \tag{27}$$

$$C_{Di} = \frac{C_L{}^2}{\pi AR\ e(\Sigma_\infty + \Sigma_s/p^2)/(\pi b^2/4)} \tag{28}$$

¶ To be published in a future issue of the Journal of Aircraft.

where the lift $L = C_L q_\infty S$ and the induced drag $D_i = C_{Di} q_\infty S$, with S being a reference wing planform area. By eliminating ϵ between Eqs. (25) and (26), and introducing $V_h = (2W/\rho A_p)^{1/2}$, we find

$$\left[\frac{V_\infty}{V_h}\right]^2 = \frac{p^4}{4[1 - p^2(1 + f/A_p)][e(p^2\Sigma_\infty + \Sigma_s)/A_p]} \tag{29}$$

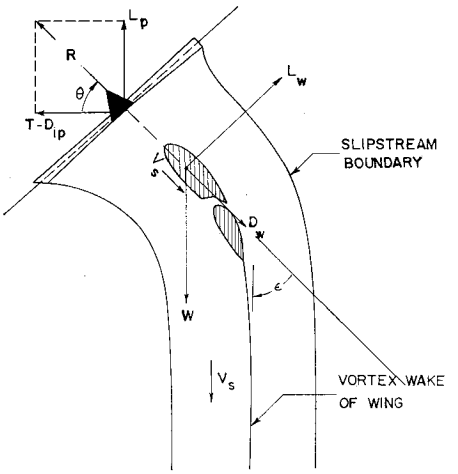

Fig. 7 Forces acting on tilt wing and deflected slipstream aircraft at hover.

Equation (17) now becomes, with p as a parameter,

$$\frac{\text{BHP}}{\text{BHP}} = \frac{2\eta_h(1-p^2)}{\eta p^3}\left[\frac{V_p}{V_s}\right]\left[\frac{V_\infty}{V_h}\right]^3 \tag{30}$$

An effective lift/drag ratio may also be calculated in this case through use of Eq. (12).

2.2.3 *Wing and propeller combinations at hover*

At hover the weight of the aircraft can either be supported entirely by the propellers (tilt-wing aircraft) or it can be divided between the propellers and the wing (deflected slipstream aircraft). We shall consider both types of aircraft, and determine the optimum division of lift between the propellers and wing-flap system at a given airplane weight (or equivalently for maximum weight at a given power).

The forces acting on the propellers and wing-flap system are shown in Fig. 7. At hover the total wing lift and drag act, respectively, perpendicular and parallel to the flow direction of the fully contracted slipstream.

For the balance of forces in the vertical and horizontal directions

$$W = L_p + L_w\cos\theta - D_w\sin\theta \tag{31}$$

$$T = D_{ip} + L_w\sin\theta + D_w\cos\theta \tag{32}$$

where L_p and $T - D_{ip}$ are given by Eqs. (21) and (22), with $\delta = \theta$ and $V_p/V_s = \frac{1}{2}$ for hover. The wing lift and drag may now be expressed as follows:

$$L_w = \rho e\Sigma_s V_s^2\sin\epsilon \tag{33}$$

$$D_w = \rho e\Sigma_s V_s^2(1-\cos\epsilon) \tag{34}$$

Note that the wing zero-lift drag has been left out of Eq. (34), since it is included in the propeller efficiency, Eq. (23). Σ_s is the cross-sectional area of the apparent mass for the flow inside the slipstream, and ϵ is the wing vortex deflection angle measured from the slipstream direction. We have here selected to write $\sin\epsilon$ for ϵ and $(1-\cos\epsilon)$ for $\epsilon^2/2$.

It is shown in Sec. B of Pt. II that $\Sigma_s = 0.3A_p$ for the optimum planar lifting system, and is independent of the number and location of the propellers at hover as long as the wing spans all of the slipstreams. For the optimum nonplanar lifting system (ducts or louvered flaps) located behind propellers, $\Sigma_s = 0.5\,A_p$, since at hover $A_p = 2A_s$.

Equations (33) and (34) are in agreement with simple momentum theory for all ϵ when ducts or louvered flaps deflect the fully contracted slipstream. The equations are valid for planar lifting systems (monoplane wing with small flaps) as long as ϵ remains small. From Eqs. (32–34) we obtain a relation between the propeller tilt angle and the wing vortex angle at infinity downstream as follows:

$$\tan\theta = \frac{1 - 2e(\Sigma_s/A_p)(1-\cos\epsilon)}{2e(\Sigma_s/A_p)\sin\epsilon} \tag{35}$$

Substitution of this expression into Eq. (31) yields after some reduction

$$\left[\frac{V_s}{V_h}\right]^4 = \frac{1}{4e^2(\Sigma_s/A_p)^2\sin^2\epsilon + [1 - 2e(\Sigma_s/A_p)(1-\cos\epsilon)]^2} \tag{36}$$

Here V_s is the true velocity at hover, and V_h is the arbitrarily defined constant velocity introduced to nondimensionalize the expression.

Thus with $P_h = \frac{1}{4}\rho\,A_p\,V_s^3$, we arrive at the following general expression:

$$\text{BHP}/\text{BHP}_h = \{4e^2(\Sigma_s/A_p)^2\sin^2\epsilon + [1 - 2e(\Sigma_s/A_p)(1-\cos\epsilon)]^2\}^{-3/4} \tag{37}$$

Equations (36) and (37) indicate that for $e = 1$, V_s/V_h and BHP/BHP_h are unity at all ϵ and θ when $\Sigma_s/A_p = 0.5$ (ducts or louvered flaps), and they give values of V_s/V_h and $\text{BHP}/\text{BHP}_h \geq 1$ when $\Sigma_s/A_p < 0.5$ (planar or semiplanar systems).

It is of interest to obtain the propeller tilt angle θ and wing vortex angle ϵ, which minimize the power required for hover. Differentiating Eq. (37) with respect to ϵ and equating the result to zero indicate that either $\epsilon = 0$ or $\Sigma_s/A_p = 0.5$ for minimum power. Now, $\epsilon = 0$ corresponds to a propeller tilt angle of 90° [from Eq. (35)], i.e., tilt-wing aircraft are optimum. The second possibility $\Sigma_s/A_p = 0.5$ occurs when we have a ducted or louvered flap system for which the downwash velocity is constant inside the slipstream. In this case simple momentum theory is valid, and the power is easily shown to be independent of the propeller tilt angle, i.e., a deflected slipstream aircraft of this type is as efficient in hover as a tilt-wing aircraft.

An alternate expression for the turning effectiveness of optimum flap systems in hover is useful for comparison with test data for which the tilt angle θ is zero, and all lift is obtained by slipstream deflection. Defining the net longitudinal (horizontal) force as $T - D_w$, and with L_w as the total lift, Eqs. (31) and (32) give

$$\text{longitudinal force/thrust} = 1 - 2e(\Sigma_s/A_p)(1-\cos\epsilon) \tag{38}$$

$$\text{lift/thrust} = 2e(\Sigma_s/A_p)\sin\epsilon \tag{39}$$

These simple relations have been plotted in Fig. 8, and are there compared with test results (from Ref. 23) on several flap systems. It is noted that nonplanar flaps are more effective than planar flaps as predicted by the theory, and that practical flap systems have values of Σ_s/A_p that lie between 0.3 (optimum planar) and 0.5 (optimum nonplanar flaps). Thus the given theoretical development appears to be well substantiated experimentally.

2.2.4 *Unified theory of wing and propeller combinations from hover to cruise speeds*

In the preceding sections expressions for minimum power required for V/STOL aircraft with unshrouded propellers have been obtained for conditions near cruise and at hover. At cruise the effects of slipstream deflection angle δ are negligible. At hover the propeller slipstream is not deflected at all (until the influence of the wing is felt). However, during the main portion of transitional flight, the propeller slipstream is deflected and encounters the wing at an appreciable angle to the flight direction. The apparent mass values obtained in Sec. B of Pt. II are based on zero upstream slipstream deflection angles. It is clear that these

values should be corrected to include the effects of slipstream deflection during transition. No such correction is available at present.

A method for obtaining the minimum power requirements throughout the transitional speed range will be developed. The method will be shown to reduce to the results of the previous sections in the hover and cruise limits. In the absence of a method for calculating the cross-sectional areas associated with apparent mass of planar wings in slipstreams having large deflection angles, the values of Σ_∞ and Σ_s for small deflection angles will be used.

Referring to Fig. 9, the force balance in the vertical and longitudinal directions yields

$$W = L_p + L_{ws}\cos\delta - D_{ws}\sin\delta + L_{w\infty} \quad (40)$$

$$T = D_{ip} + L_{ws}\sin\delta + D_{ws}\cos\delta + D_{w\infty} + fq_\infty \quad (41)$$

where L_p and $T - D_{ip}$ are given by Eqs. (21) and (22). The wing lift and drag may now be expressed as follows:

$$L_{ws} = \rho V_s^2 e\Sigma_s \sin\epsilon \quad (42)$$

$$L_{w\infty} = \tfrac{1}{2}\rho V_\infty^2 e\Sigma_\infty [2 - \sin^2(\delta + \epsilon)]\sin(\delta + \epsilon) \quad (43)$$

$$D_{ws} = \rho V_s^2 e\Sigma_s(1 - \cos\epsilon) \quad (44)$$

$$D_{w\infty} = \tfrac{1}{2}\rho V_\infty^2 e\Sigma_\infty \sin^2(\delta + \epsilon)\cos(\delta + \epsilon) \quad (45)$$

The deflection angle of the vortex sheet outside the slipstreams equals the sum of the slipstream deflection angle and that of the vortex sheet inside the slipstream, i.e., $\delta + \epsilon$. Thus the trailing vortex sheet makes a constant angle $\delta + \epsilon$ with the horizontal direction along the entire span in accordance with the criterion for minimum induced drag.

Substitution of Eqs. (21, 22, and 42–45) into Eqs. (40) and (41) and introduction of V_h give

$$(V_h/V_\infty)^2 = (2/p^2)\{(A_s/A_p)(1 - e\Sigma_s/A_s)\sin\delta + e(\Sigma_s/A_p)\sin(\delta + \epsilon) + (\tfrac{1}{2})p^2 e(\Sigma_\infty/A_p) \times [2 - \sin^2(\delta + \epsilon)]\sin(\delta + \epsilon)\} \quad (46)$$

$$[e(\Sigma_s/A_s)\cos(\delta + \epsilon) - p](A_s/A_p) = -(A_s/A_p)(1 - e\Sigma_s/A_s)\cos\delta + (p^2/2)[e(\Sigma_\infty/A_p)\sin^2(\delta + \epsilon)\cos(\delta + \epsilon) + f/A_p] \quad (47)$$

These equations must be solved simultaneously for V_∞/V_h and $(\delta + \epsilon)$ in terms of the parameter p. However, before this can be done the propeller tilt angle schedule, θ vs p, must be determined so that δ becomes a known function of p. The optimum tilt angle schedule (the θ vs p that minimizes the power required) will be found below for p small. It is recalled that Sec. 2.2.3 gave $\theta_{opt} = \delta = \pi/2$ for $p = 0$.

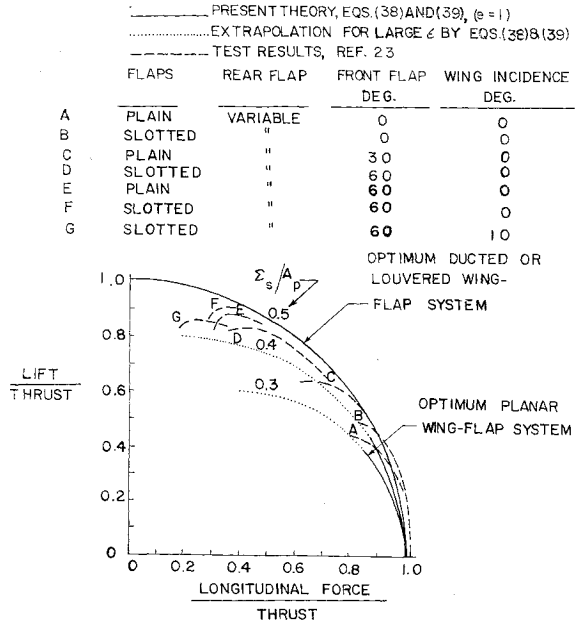

Fig. 8 Comparison of static turning effectiveness of wing and propeller combinations. Test results on wing-propeller combinations with plain and slotted flaps. Untilted propeller ($\theta = 0$).

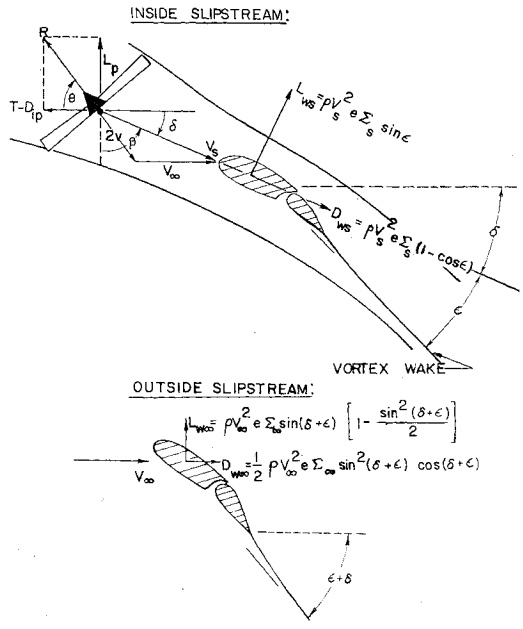

Fig. 9 Forces acting on tilt-wing and deflected slipstream aircraft during transition (unified theory).

For $p \ll 1$ we take $\delta = (\pi/2) - \beta$ (see Fig. 9), $\cos\delta = \beta$, $\sin\delta = 1 - \beta^2/2$, and $\cos\theta = (\pi/2) - \theta$, where β and p are assumed to be of comparable order of magnitude. To the first order in β and p, Eq. (20) gives

$$\beta = p + \cos\theta = p + [(\pi/2) - \theta] \quad (48)$$

From Eq. (19), to the same order in β and p, and using the previous result,

$$\sin\delta = [1 - (p^2/2) - p(\beta - p)]\sin\theta \simeq \sin\theta \quad (49)$$

Equation (16), to second order in β and p, becomes

$$V_p/V_s = \tfrac{1}{2}[1 + \tfrac{1}{2}(p^2 + 2p\beta)] \quad (50)$$

Substituting into Eq. (47) and taking $\sin\epsilon = \epsilon$ and $\cos\epsilon = 1$ gives to lowest order

$$\beta = 2e(\Sigma_s/A_p)\epsilon + p \quad (51)$$

Next, we substitute Eqs. (50) and (51) into Eq. (46), retaining only terms up to and including order two in ϵ and p. The resultant expression is then differentiated with respect to ϵ for a fixed forward speed and aircraft weight (V_∞ and V_h const). The derivatives $dp/d\epsilon$ are set equal to zero corresponding to the minimum value of V_s. This is equivalent to minimizing the power required, as may be seen from Eq. (30), provided V_p is only weakly dependent on β. The resulting optimum value of ϵ is found to be

$$\epsilon_{opt} = \frac{p}{1 - 2e\Sigma_s/A_p} \quad (52)$$

and by Eq. (51) we have the particularly simple result

$$\epsilon = \beta \quad (53)$$

In terms of θ, through use of Eq. (48), the optimum propeller tilt angle schedule becomes

$$\theta_{opt} = \frac{\pi}{2} - \frac{2pe\Sigma_s/A_p}{1 - 2e\Sigma_s/A_p} = (\pi/2) - (3p/2) \quad (54)$$

when $\Sigma_s/A_p = 0.3$ and $e = 1$.

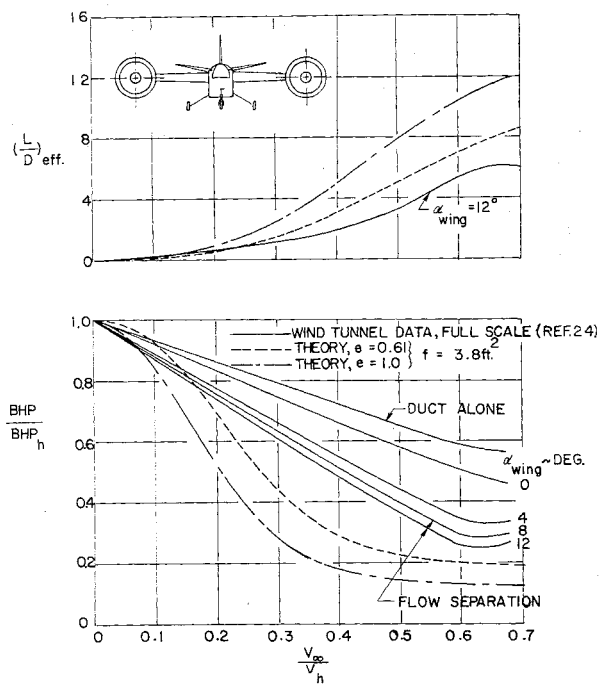

Fig. 10 Doak VZ-4DA. Correlation of wind-tunnel data with theory (constant altitude; linear fall-off of propeller efficiency: $\eta_h = 0.74$, $\eta_{\text{cruise}} = 0.62$).

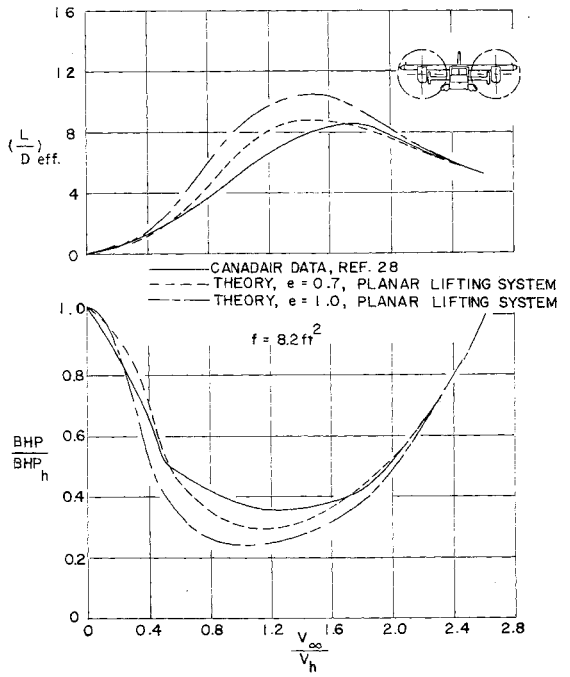

Fig. 12 Canadair CL-84A. Correlation of Canadair data with theory (constant altitude and propeller efficiency).

Although Eq. (54) is only valid for small p, it leads to a negligibly small value of θ_{opt} at $p \simeq 1$ consistent with cruise conditions. In order to simplify the transitional theory as much as possible, Eq. (54) will be employed throughout the flight regime. It is recognized that for wings of relatively small chord, this schedule may result in unrealistically high C_L's, and that an alternate constant C_L schedule may be required. No corresponding schedule is needed for the optimum nonplanar lifting system (louvered or ducted flaps). Reference to Eq. (52) indicates that ϵ_{opt} is undefined for this case. This is the same result as was obtained at hover.

Using the previous tilt angle schedule, Eqs. (46) and (47) may be solved for BHP/BHP$_h$ vs V_∞/V_h.

3. Correlation with Test Results

The theory developed in the preceding pages has been used to calculate the lift/drag ratio and nondimensional power required of several V/STOL aircraft as functions of nondimensional velocity. One ducted and five unshrouded propeller aircraft have been considered.[24–31] The calculated curves are compared with existing data from these references

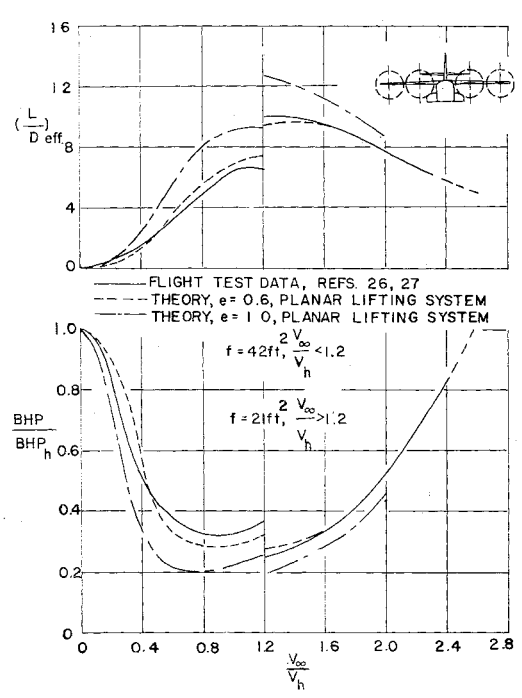

Fig. 11 Vought XC-142A. Correlation of flight test data with theory (constant altitude and propeller efficiency).

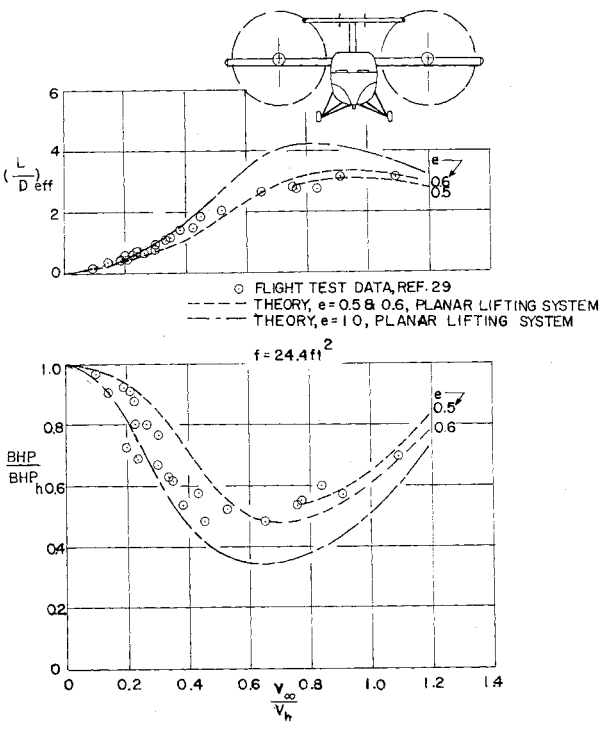

Fig. 13 Vertol VZ-2. Correlation of flight test data wit theory (constant altitude and propeller efficiency).

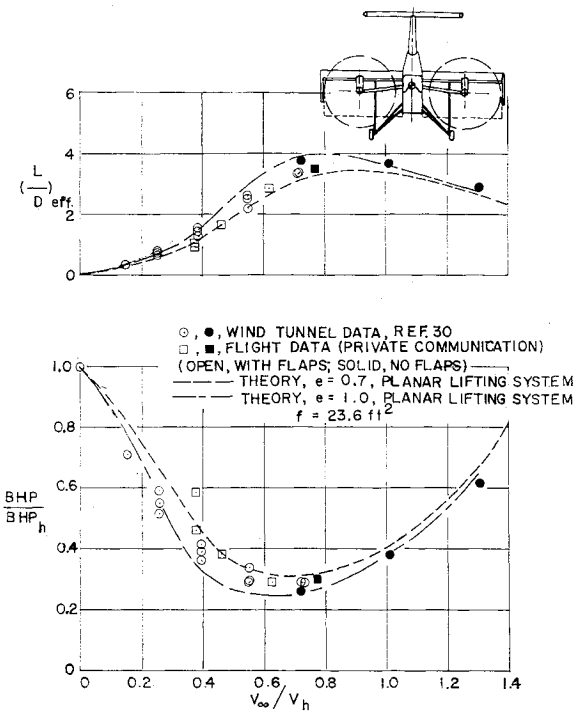

Fig. 14 Ryan VZ-3. Correlation of flight test and wind-tunnel data with theory (constant altitude; linearly increasing propeller efficiency: $\eta_h = 0.44$, $\eta = 0.65$ at $V_\infty/V_h \geq 0.5$).

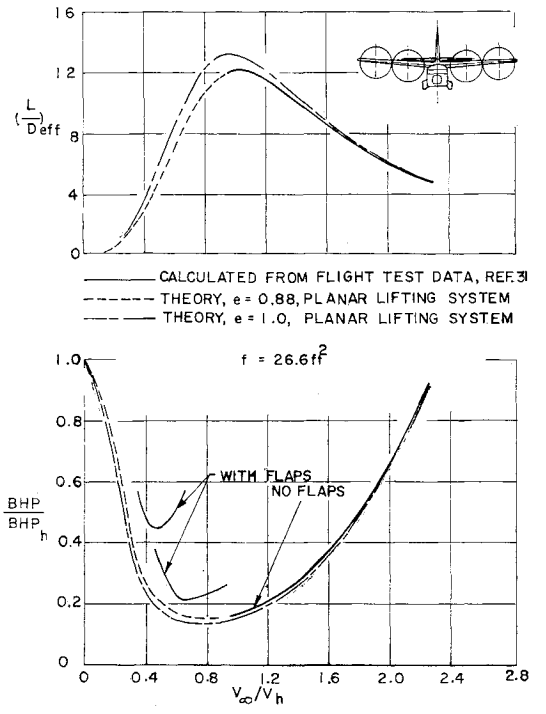

Fig. 15 Breguet 941. Correlation of flight test data with theory (constant altitude and propeller efficiency).

in Figs. 10–15. A planar lifting system was assumed for the unshrouded configurations.

Using $e = 1.0$ leads to generally lower values of BHP/BHP$_h$ and larger values of $(L/D)_{\text{eff}}$ over the entire speed range than shown by the test data, and indicates the relative size of the over-all improvements in aircraft range and endurance which would be possible if, by design modifications, the optimum theoretical wing effectiveness could be achieved in flight.

To assess the aerodynamic effectiveness of the various V/STOL aircraft considered, calculations were also carried out for several values of $e < 1$. As seen from the figures, a wing effectiveness value that agreed with the test data at cruise did not necessarily show agreement during transition.

The different propeller tilt angle schedules used during flight test, as compared with the schedule used in the calculations, will also influence the power required during transition and thereby cause an apparent change in e. Also, inherent deficiencies in both the large-deflection propeller slipstream theory and the large-angle vortex wake theory could produce an apparent change in wing effectiveness. For these reasons the meaning of the apparent flight test value of e during transition is not altogether clear.

It should also be pointed out that the flowfield around an aircraft depends on a great many factors, only a few of which have been incorporated into the theory. For instance, effects of flow separation might well play a dominant role under some circumstances. Also, the large camber effect due to flap deployment mentioned previously may be of significance during transition. Good agreement between theory and test results presupposes that the factors omitted in the theory have a negligible influence on the flowfield. It is with these reservations that theory and test results have been correlated.

4. Conclusions

In the previous sections a unified self-consistent performance theory for V/STOL aircraft has been presented. The theory is valid at all forward speeds, and allows rapid determination of lift/drag ratios and nondimensional power required vs nondimensional speed for any tilt-wing and deflected slipstream aircraft in equilibrium level flight.

The development is based upon classical aerodynamic theory as recently extended to large vortex wake angles and takes into account wing interaction with multiple propellers and ducted fans. The important cross-sectional area parameter associated with apparent mass has been determined for a number of general configurations of both shrouded and unshrouded propeller V/STOL aircraft. The theory has been correlated with available experimental data on six different aircraft, and shows realistic agreement.

References

[1] Munk, M., "Isoperimetrische Aufgaben aus der Theorie des Fluges," Inaug. Dissertation, Univ. of Gottingen, Gottingen, Germany (1919).

[2] Helmbold, H. B., "Limitations of circulation lift," J. Aeronaut. Sci. **24**, 237–238 (1957).

[3] Ribner, H. S., "On the lift and induced drag associated with large angles," Institute Aerosphysics, Univ. of Toronto, UTIA 19 (January 1958).

[4] McCormick, B. W., "The limiting circulatory lift of a wing of finite aspect ratio," J. Aerospace Sci. **26**, 247–248 (1959).

[5] Hancock, G. J., "Comments on 'Limiting circulatory lift of a wing of finite aspect ratio'," J. Aerospace Sci. **27**, 65–66 (1960).

[6] Davenport, F. J., "A further discussion of the limiting circulatory lift of a finite-span wing," J. Aero/Space Sci. **27** (December 1960).

[7] Cone, C. D., "A theoretical investigation of vortex-sheet deformation behind a highly loaded wing and its effect on lift," NASA TN D-657 (April 1961).

[8] Graham, E. W., "Notes on jet impingement and on the limiting lift for a finite aspect ratio wing," Boeing Scientific Research Labs., TM 34 (August 1964).

[9] Spreiter, J. R., "The aerodynamic forces on slender plane— and cruciform—wing and body combinations," NACA Rept. 962 (March 1949).

[10] Durand, W. F., *Aerodynamic Theory*, edited by W. F. Durand (Springer-Verlag, Berlin, 1935), Vol. II.

[11] Koning, C., "Influence of the propeller on other parts of the airplane structure," *Aerodynamic Theory*, edited by W. F. Durand (Springer-Verlag, Berlin, 1935), Vol. IV.

[12] Glauert, H., "The lift and drag of a wing spanning a free jet," British Aeronautical Research Council R & M 1603 (1934).

[13] Smelt, R. and Davies, H., "Estimation of increase in lift due to slipstream," British Aeronautical Research Council R & M 1788 (1937).

[14] Franke, A. and Weinig, F., "Tragflugel and Schraubenstrahl," Luftfahrtforschung **15,** No. 6 (1938); also NACA TM 920 (1939).

[15] v. Baranoff, V., "Effect of the propeller slipstream on downwash," Luftfahrtforschung, British RTP Translation 1555 (January 20, 1942).

[16] Squire, H. B. and Chester, W., "Calculation of the effect of slipstream on lift and induced drag," British Aeronautical Research Council R & M 2368 (1945).

[17] Graham, E. W., Lagerstrom, P. A., Licher, R. M., Beane, B. J., "A preliminary theoretical investigation of the effects of propeller slipstream on wing lift," Douglas Aircraft Co. Rept. SM-14991 (1953).

[18] Rethorst, S. C., "Characteristics of an airfoil extending through a circular jet," Guggenheim Aeronautical Lab., California Institute of Technology, Pasadena, Calif., Ph.D. Thesis (1956).

[19] Ribner, H. S., "Theory of wings in slipstreams," Institute of Aerophysics, Univ. of Toronto, UTIA Rept. 60 (May 1959).

[20] Kuhn, R. E., "Semiempirical procedure for estimating lift and drag characteristics of propeller-wing-flap configurations for vertical- and short-take-off- and-landing airplanes," NASA MEMO 1-16-59L (February 1959).

[21] Ribner, H. S. and Ellis, N. D., "Theory and computer study of a wing in a slipstream," AIAA Paper 66-466 (June 1966).

[22] Karman and Tsien, "Lifting line theory for a wing in non-uniform flow," Quart. Appl. Math. **3,** 1 (April 1945).

[23] Kuhn, R. E. and Draper, J. W., "Investigation of effectiveness of large-chord slotted flaps in deflecting propeller slipstreams downward for vertical take-off and low-speed flight," NACA TN 3364 (January 1955).

[24] Goodson, K. W. and Grunwald, J. J., "Aerodynamic characteristics of a powered semispan tilting-shrouded-propeller VTOL model in hovering and transition flight," NASA TN D-981 (January 1962).

[25] Mort, K. W. and Yaggy, P. F., "Aerodynamic characteristics of a 4-foot-diameter ducted fan mounted on the tip of a semispan wing," NASA TN D-1301 (April 1962).

[26] Leppert, D. S., "Model XC-142A aircraft flight test summary," Rept. 6, Ling Temco Vought Rept. 2-59110/4R-967 (January 8, 1965).

[27] Chaplin, H. R., Private communication, David Taylor Model Basin (February 16, 1966).

[28] Phillips F. C., Private communication Canadair Limited, Program Manager CL-84 (December 22, 1965).

[29] Pegg, R. J., Kelley, H. L., and Reeder, J. P., "Flight investigation of the VZ-2 tilt-wing aircraft with full span flap," NASA TN D-2680 (March 1965).

[30] James, H. A., Wingrove, R. C., Holzhauser, C. A., and Drinkwater, F. J., "Wind tunnel and piloted flight simulator investigation of a deflected-slipstream VTOL airplane, the Ryan VZ-3RY," NASA TN D-89 (November 1959).

[31] Quigley, H. C., Inis, R. C., and Holzhauser, C. A., "A flight investigation of the performance, handling qualities, and operational characteristics of a deflected slipstream STOL transport airplane having four interconnected propellers," NASA TN D-2231 (March 1964).